Astron. Astrophys. 343, 163–174 (1999)
Beskrovnaya, N.G., Pogodin, M.A., Miroshnichenko, A.S., Savanov, I.G., Shakhovskoy, N.M., Rostopchina, A.N., Kozlova, O.B., Kuratov, K.S. 1999. A&A, 343, 163-174. Spectroscopic, photometric, and polarimetric study of the Herbig Ae candidate HD 36112
Made available courtesy of EDP Sciences: http://aa.springer.de/bibs/9343001/2300163/small.htm

ASTRONOMY AND ASTROPHYSICS

Spectroscopic, photometric, and polarimetric study of the Herbig Ae candidate HD 36112

N.G. Beskrovnaya[1], M.A. Pogodin[1], A.S. Miroshnichenko[1], P.S. Thé[2], I.S. Savanov[3], N.M. Shakhovskoy[3], A.N. Rostopchina[3], O.V. Kozlova[3], and K.S. Kuratov[4]

[1] Central Astronomical Observatory of the Russian Academy of Sciences at Pulkovo, 196140 Saint-Petersburg, Russia (e-mail: beskr@pulkovo.spb.su)
[2] Universiteit van Amsterdam, Astronomical Institute, Kruislaan 403, 1098 SJ Amsterdam, The Netherlands
[3] Crimean Astrophysical Observatory, 334413 Nauchnyi, Crimea, Ukraine
[4] Fesenkov Astrophysical Institute of the Kazakhstan National Academy of Sciences, 480068 Almaty, Kazakhstan

Received 5 January 1998 / Accepted 9 October 1998

Abstract. We describe observations of the Herbig Ae candidate HD 36112 including high-resolution spectroscopy of photospheric and circumstellar lines, multi-colour photometry and polarimetry. These observations reveal that many features of the observational appearance of HD 36112 are similar to those of 'classical' Herbig Ae stars. Among these are: the far IR excess, manifestations of the high-temperature zone in the inner envelope, distinctive types of the Hα profile variations, and variable multi-component polarization and brightness parameters.

The fundamental characteristics of the star have been determined. In particular, HD 36112 proves to be an unreddened A8 V of age $t \sim 5 \div 10 \times 10^6$ years. This means, that the star is still at the PMS phase of evolution, but close to the ZAMS. The anomalous abundances of barium and silicon discovered in HD 36112 allow to suggest that chemical anomalies can arise already at the early stages of stellar evolution.

The totality of observed properties of HD 36112 give evidence of complicated structure of the gaseous-dusty envelope around this object, including the variable stellar wind with an extended acceleration zone, as well as large and small-grained dust, located in the orthogonal planes.

Key words: stars: individual: HD 36112 – line: profiles – polarization – stars: circumstellar matter – stars: mass-loss – stars: pre-main sequence

1. Introduction

The Ae-star HD 36112 (MWC 758, $V = 8\overset{\mathrm{m}}{.}3$) remained, until recent time, one of the poorly studied bright emission-line object. Its spectral type was estimated as A3 in the HD catalogue. Zuckerman et al. (1995) detected a CO maser in the vicinity of HD 36112 and quoted its spectral type as A5e IV. After the star had been identified with an *IRAS* PSC source 05273+2517 (Dong & Hu 1991, Oudmaijer et al. 1992), Thé et al. (1994) included it in their enlarged catalogue as a candidate Herbig Ae/Be star (Herbig 1960) with a large IR excess due to radiation of cool circumstellar dust with the temperature $T \sim 150$ K.

HD 36112 is located in the Taurus–Auriga complex of dark clouds where a few more bright stars with similar IR excesses have been found. They form a chain along the projection of the galactic equator with declinations from $+24^\circ$ to $+31^\circ$. Among them there are three well–known Herbig Ae/Be stars (AB Aur, CQ Tau, and RR Tau) and three Herbig Ae candidates (HD 32509, HD 35187, and HD 31648).

Pogodin (1995) obtained the first high-resolution spectra of HD 36112 in the Hα region during three consecutive nights in January, 1994. The Hα profile underwent variations similar to those detected in some Herbig Ae stars, when a classical P Cyg profile transforms into a single symmetric peak during one day (Beskrovnaya et al. 1991, 1995). After this, in 1994–1996, a complex programme of detailed spectral, photometric, and polarimetric study of this object has been carried out. This investigation revealed many unusual properties of HD 36112 which are presented in this paper.

2. Observational programme

2.1. Spectroscopy in the regions containing photospheric lines

These observations were performed in order to refine such fundamental characteristics of the star as effective temperature, $T_{\rm eff}$, surface gravity, $\log g$, chemical abundances, and projected rotational velocity, $V \sin i$. The following lines were observed: Si II $\lambda\lambda$ 6347 and 6371, Ca I$\lambda\lambda$ 6122, 6439 and 6463, Ba II$\lambda\lambda$ 5854, 6142 and 6497, as well as a number of lines of Fe I, O I, etc. Additionally, they were used to check for a possible binarity of the object, which can be a cause of its spectral variability.

2.2. Investigation of the rapid variability of the lines forming in the gaseous envelope

This was the main direction of our programme. It was carried out within the framework of a complex programme of the study

Send offprint requests to: N.G. Beskrovnaya

of circumstellar peculiarities in young early–type stars and was aimed at reconstructing the kinematic structure of the circumstellar gaseous envelope on the basis of the data on rapid ($\tau \sim$ days, hours) variability of line profiles forming at different distances from the star. The following lines were selected for this study: He I λ 5876 (high-temperature zone near the star), DNa I $\lambda\lambda$ 5889, 5895 (remote part of the envelope, $r \gtrsim 10R_*$), and Hα (forming throughout the envelope). Additionally, a few spectrograms were obtained in the region of Hβ line.

2.3. Multicolour photometry and polarimetry

Measurements of the linear polarization parameters in the $UBVRI$ passbands of the Johnson system accompanied the spectroscopic observations. This provides additional independent parameters of the circumstellar medium, including both dusty and gaseous envelopes.

Photometry in the optical and near IR spectral domains was performed to separate processes taking place on the star itself and in the envelope and to measure (if present) the IR excess in the region of 1–3 μm.

3. Data acquisition and reduction

3.1. Spectroscopic observations

The spectroscopic observations of HD 36112 were collected between December 1994 and January 1996 at the Crimean Astrophysical Observatory. The 2.6m Shajn telescope equipped with a CCD-detector placed in the first camera of the coudé–spectrograph was used yielding a spectral resolving power $R \sim 30\,000$ and a signal-to-noise ratio $S/N \sim 50 \div 120$ at the continuum level. An *A*stromed CCD–2000 (Huovelin et al. 1986) providing the wavelength coverage, $\Delta\lambda$, of about 30 Å was in use until mid–1995. Then a new detector – SDS–9000 ''Photometric GmbH" – was mounted and $\Delta\lambda$ became larger ($\sim$ 65 Å).

Seventy seven spectra have been obtained in six spectral regions encompassing the following lines: Hα, Hβ, He I λ 5876 and DNa I (centered at λ 5875Å), and, finally, a number of photospheric lines (in three spectral intervals centered at $\lambda\lambda$ 6130, 6360, and 6470 Å). Data reduction followed the standard procedures and was done with the SPE code developed at the Crimean Observatory by S.G. Sergeev.

The spectra near Hα and λ 5885 Å were taken several times during each night with a mean S/N ratio of about 70 and 85, respectively. In other regions, 1–2 observations were made in each observing run. Tables 1 and 2 present the observing dates and basic parameters of the emission profiles for the Hα (Table 1), He I λ 5876 and DNa I (Table 2). The remaining spectra are listed in Table 3.

3.2. Polarimetric observations

The $UBVRI$ polarimetric observations of HD 36112 were collected systematically from December, 1994 to January, 1996 at the Crimean Astrophysical Observatory. The five-channel

Table 1. The log of spectral observations in the Hα region and some parameters of the emission profiles. The estimated uncertainties ($\pm\sigma$) are presented at the bottom.

Date	UT	V_b	V_e	V_0	V_r	$F_\mathrm{max}/F_\mathrm{c}$
	$16^\mathrm{h}08^\mathrm{m}$	−375	−6	+20	330	3.00
24/25	$17^\mathrm{h}15^\mathrm{m}$	−390	−7	+16	360	3.02
XII.94	$18^\mathrm{h}30^\mathrm{m}$	−400	−6	+21	360	3.00
	$21^\mathrm{h}32^\mathrm{m}$	−400	−3	+24	350	3.01
	$1^\mathrm{h}10^\mathrm{m}$	−380	−5	+25	360	3.00
	$2^\mathrm{h}38^\mathrm{m}$	−400	−4	+26	350	3.02
	$15^\mathrm{h}24^\mathrm{m}$	−370	+19	+34	340	3.08
	$16^\mathrm{h}33^\mathrm{m}$	−390	+19	+34	360	3.03
	$17^\mathrm{h}05^\mathrm{m}$	−370	+20	+35	340	3.03
29/30	$18^\mathrm{h}22^\mathrm{m}$	−370	+20	+38	380	3.02
XII.94	$19^\mathrm{h}24^\mathrm{m}$	−365	+22	+40	340	3.05
	$23^\mathrm{h}17^\mathrm{m}$	−375	+25	+47	335	3.09
	$0^\mathrm{h}24^\mathrm{m}$	−400	+23	+43	330	3.05
	$1^\mathrm{h}30^\mathrm{m}$	−380	+23	+43	365	3.04
	$2^\mathrm{h}33^\mathrm{m}$	−360	+23	+43	340	3.04
	$17^\mathrm{h}22^\mathrm{m}$	−350	+19	+41	350	2.93
30/31	$18^\mathrm{h}25^\mathrm{m}$	−400	+18	+39	350	2.86
XII.94	$19^\mathrm{h}28^\mathrm{m}$	−415	+14	+34	340	2.86
	$22^\mathrm{h}57^\mathrm{m}$	−410	+10	+32	315	2.79
	$0^\mathrm{h}00^\mathrm{m}$	−450	+10	+30	320	2.72
	$1^\mathrm{h}02^\mathrm{m}$	−450	+ 9	+32	315	2.58
6/7	$15^\mathrm{h}43^\mathrm{m}$	−410	−12	+10	330	2.94
I.95	$18^\mathrm{h}58^\mathrm{m}$	−420	−10	+14	313	3.02
25/26 II.95	$21^\mathrm{h}00^\mathrm{m}$	−315	+ 5	+ 8	270	3.12
4/5 III.95	$16^\mathrm{h}58^\mathrm{m}$	−305	+ 3	+16	310	2.76
5/6 XI.95	$20^\mathrm{h}39^\mathrm{m}$	−410	+12	+54	415	3.06
	$16^\mathrm{h}07^\mathrm{m}$	−405	−3	+20	385	3.82
	$18^\mathrm{h}29^\mathrm{m}$	−400	−2	+17	400	3.83
9/10	$22^\mathrm{h}05^\mathrm{m}$	−370	−3	+16	390	3.81
I.96	$23^\mathrm{h}10^\mathrm{m}$	−355	−4	+14	390	3.82
	$0^\mathrm{h}03^\mathrm{m}$	−380	−2	+14	390	3.83
	$0^\mathrm{h}56^\mathrm{m}$	−400	−1	+11	390	3.81
	$2^\mathrm{h}04^\mathrm{m}$	−405	−4	+10	390	3.81
	$20^\mathrm{h}02^\mathrm{m}$	−415	−3	0	370	3.74
10/11	$21^\mathrm{h}34^\mathrm{m}$	−415	−2	+ 1	350	3.67
I.96	$22^\mathrm{h}59^\mathrm{m}$	−435	−5	0	360	3.74
	$1^\mathrm{h}57^\mathrm{m}$	−435	−8	−3	340	3.62
11/12 I.96	$19^\mathrm{h}01^\mathrm{m}$	−370	+ 2	+23	410	3.57
$\pm\sigma$		10	1	1	10	0.01

V_e – the radial velocity of the emission maximum F_max;
V_0 – the radial velocity of the line centre of gravity;
V_b and V_r – the positions of the blue and red edges of the emission line, respectively.

Table 2. The same as Table 1, but for the λ 5885 Å region

		He I λ 5876				DNa I		
Date	UT	V_b	V_e	V_0	V_r	V_b	V_e	V_r
	16^h45^m	−250	−29	−14	210	−380	−37	100
	17^h52^m	−275	−25	−16	250	−370	−40	110
24/25	20^h58^m	−275	−25	−16	250	−400	−39	90
XII.94	21^h38^m	−280	−26	−19	215	−390	−38	85
	1^h42^m	−300	−30	−14	240	−380	−41	95
	3^h10^m	−270	−28	−20	220	−400	−40	100
	16^h01^m	−300	0	−12	280	−380	−15	130
	17^h50^m	−290	+1	−8	265	−390	−18	90
29/30	18^h53^m	−290	−3	−10	260	−390	−17	110
XI.94	23^h52^m	−300	−1	−10	250	−370	−16	120
	0^h56^m	−280	+2	−7	270	−365	−18	100
	2^h02^m	−300	−5	−12	260	−380	−17	90
	17^h53^m	−310	−33	−43	215	−385	−35	90
30/31	18^h57^m	−350	−35	−50	230	−380	−30	80
XI.94	19^h59^m	−340	−34	−48	225	−375	−32	100
	23^h28^m	−350	−32	−48	225	−365	−31	120
	0^h31^m	−330	−34	−51	220	−370	−30	110
06/07	16^h25^m	−275	−126	−77	215	−370	−52	90
I.95	18^h07^m	−285	−132	−81	205	−350	−48	100
05/06	21^h40^m	−300	−11	+6	311	−270	*–	112
XI.95							–	
	17^h30^m	−190	+7	+13	230	−400	–	150
	20^h12^m	−300	+2	−3	260	−390	–	115
09/10	22^h38^m	−220	+3	+2	220	−400	–	170
I.96	23^h36^m	−200	+10	+13	260	−340	–	150
	0^h30^m	−250	+9	+10	260	−400	–	140
	1^h28^m	−230	+5	0	230	−340	–	150
	20^h33^m	−280	−7	−25	215	−390	–	130
10/11	22^h01^m	−350	−16	−36	250	−360	–	140
I.96	23^h25^m	−300	−13	−35	210	−385	–	140
	1^h31^m	−300	−18	−38	200	−385	–	160

* The peak is distorted by the IS absorption.

photometer-polarimeter of the Helsinki University Observatory (Piirola 1975) attached to the 1.25m telescope was used. This instrument enables the polarization of an object to be monitored simultaneously in five passbands close to the standard Johnson $UBVRI$ system. The aperture of $10''$–$20''$ was used depending on seeing conditions. The exposure time was 10 s, resulting in 3.5 min being necessary for one polarimetric measurement. The sky background was recorded every 15 minutes for 30 seconds and then interpolated and subtracted from every 10 s integration in each channel. In processing the data a correction was applied for instrumental polarization by measurements of unpolarized stars listed by Serkowski (1974). The normalized Stokes parameters ($q = Q/I$ and $u = U/I$) were computed for each individual measurement and then averaged (as the weighted mean) for each observing night. When there was a gap in monitoring during a night, two or more values per night were obtained, each being the weighted mean value for corresponding continuous series. The log of polarimetric observations together with the polarization parameters obtained for each date (the percentage $P\% = \sqrt{q^2 + u^2}$ and the position angle $\theta = 0.5 \arctan q/u$) are presented in Table 4.

Table 3. The list of spectra encompassing Hβ and photospheric lines

Date	Band, λ (Å)	UT	S/N
29/30.12.94	6130	16^h45^m	120
4/5.03.95	6130	17^h45^m	92
5/6.11.95	4861	02^h21^m	67
9/10.01.96	4861	21^h02^m	63
	6130	19^h59^m	98
	6360	19^h28^m	96
	6470	20^h55^m	69
10/11.01.96	6130	0^h08^m	125
	6360	1^h33^m	145
	6470	3^h32^m	125

3.3. Photometric observations

The photometric observations of HD 36112 were carried out between January, 1993 and December, 1996 with the two 1m telescopes (Assy Observatory and Tien-Shan Observatory) of the Fesenkov Astrophysical Institute of the National Academy of Sciences of Kazakhstan, equipped with the two-channel photometer-polarimeter (Bergner et al. 1988). A GaAs photomultiplier was used to measure count rates in the Johnson $UBVRI$ passbands. During eight nights the JHK observations were performed with the use of a PbS detector simultaneously with the $UBVRI$ photometry. Two additional observations were carried out in March 1993 at the 1.25m telescope of the Sternberg Astronomical Institute in Crimea with the infrared photometer equipped with an InSb photomultiplier as a detector (Nadzhip 1986). The comparison stars were: HD 36546 in the optical region, and β Tau in the infrared region. The results of the $UBVRI$ photometric observations are presented in Table 5. Typical errors of these measurements are $0\overset{m}{.}01$–$0\overset{m}{.}02$. The results of IR photometry together with the estimated uncertainties are given in Table 6.

4. Results

4.1. Photometry

As it is seen in Tables 5 and 6, HD 36112 seems to exhibit irregular photometric variations in all the passbands with the peak-to-peak amplitude not exceeding $0\overset{m}{.}2$ in $UBVRIJH$ and somewhat higher in the K passband. The only photoelectric measurement of HD 36112 obtained so far (in the Strömgren

Table 4. Weighted nightly mean linear polarization parameters of HD 36112. N is the number of individual measurements in each data point, σ_p and σ_θ are the estimated errors of the weighted mean values of the polarization degree and of the position angle, respectively.

Date/ JD2400000+	N	Band	P, %	σ_p, %	θ,°	σ_θ,°	Date/ JD2400000+	N	Band	P, %	σ_p, %	θ,°	σ_θ,°
24.12.94	20	U	0.408	0.038	50.58	2.68	09:01:96	44	U	0.286	0.030	63.97	2.97
49711.3239		B	0.244	0.017	47.95	2.04	50092.5213		B	0.271	0.015	63.25	1.55
		V	0.243	0.029	40.70	3.38			V	0.196	0.017	64.86	2.54
		R	0.166	0.025	34.61	4.27			R	0.140	0.012	70.58	2.46
		I	0.083	0.022	33.93	7.48			I	0.113	0.019	95.39	4.67
06.01.95	40	U	0.301	0.043	31.39	4.07	10:01:96	8	U	0.367	0.045	57.75	3.48
49724.2447		B	0.174	0.023	10.09	3.74	50093.3018		B	0.271	0.036	59.39	3.76
		V	0.199	0.030	173.78	4.28			V	0.357	0.033	58.72	2.67
		R	0.285	0.021	171.79	2.08			R	0.157	0.031	61.04	5.65
		I	0.337	0.031	165.88	2.60			I	0.091	0.031	51.19	9.33
21:01:95	20	U	0.222	0.087	66.32	10.70	10:01:96	2	U	0.285	0.116	68.04	11.04
49739.2687		B	0.117	0.044	37.28	10.20	50093.3178		B	0.309	0.037	64.79	3.37
		V	0.090	0.057	79.06	16.15			V	0.447	0.142	50.99	8.82
		R	0.108	0.041	2.17	10.28			R	0.191	0.016	50.51	2.36
		I	0.144	0.039	163.25	7.58			I	0.040	0.007	30.08	4.80
30:01:95	4	U	0.241	0.137	40.65	14.81	10:01:96	52	U	0.371	0.020	54.75	1.51
49748.1990		B	0.063	0.071	30.65	24.23	50093.5001		B	0.311	0.014	56.14	1.30
		V	0.105	0.047	63.97	12.05			V	0.253	0.016	55.27	1.81
		R	0.040	0.124	46.74	36.06			R	0.169	0.010	58.61	1.72
		I	0.039	0.104	59.95	34.70			I	0.084	0.013	58.97	4.30
13:02:95	16	U	0.143	0.047	57.51	9.09	11:01:96	8	U	0.391	0.027	58.52	1.94
49762.3423		B	0.099	0.030	81.14	8.45	50094.4004		B	0.258	0.032	54.15	3.59
		V	0.081	0.030	138.89	10.14			V	0.268	0.026	51.08	2.78
		R	0.105	0.021	143.48	5.64			R	0.160	0.018	54.18	3.16
		I	0.234	0.026	149.59	3.21			I	0.110	0.034	23.35	8.54
05:11:95	31	U	0.237	0.032	60.05	3.82	12:01:96	4	U	0.337	0.075	60.61	6.28
50027.4066		B	0.146	0.011	51.62	2.25	50095.2468		B	0.323	0.028	52.34	2.49
		V	0.180	0.026	34.84	4.17			V	0.205	0.074	48.27	9.88
		R	0.083	0.018	21.45	6.26			R	0.179	0.042	59.93	6.64
		I	0.114	0.022	170.65	5.54			I	0.048	0.059	73.20	25.33
25:11:95	8	U	0.462	0.044	61.03	2.72	12:01:96	7	U	0.338	0.060	55.62	5.03
50047.3085		B	0.311	0.021	49.74	1.93	50095.4071		B	0.282	0.031	47.52	3.17
		V	0.251	0.035	37.72	4.00			V	0.215	0.054	54.31	7.05
		R	0.145	0.029	26.20	5.71			R	0.202	0.037	50.48	5.15
		I	0.215	0.032	9.73	4.27			I	0.113	0.028	54.58	6.95
09:01:96	4	U	0.344	0.038	64.59	3.14							
50092.2688		B	0.172	0.027	56.94	4.42							
		V	0.132	0.051	64.96	10.53							
		R	0.129	0.031	77.14	6.67							
		I	0.047	0.045	149.70	21.89							

system) has been published by Perry & Johnston (1982). This result transformed into the Johnson system ($V = 8\overset{\mathrm{m}}{.}31, B - V = 0\overset{\mathrm{m}}{.}24$) coincides with our data. Results of the infrared photometry by Bogaert (1994) presented in Table 6 are also very close to our data.

The mean colour indices of HD 36112, $(B-V) = 0\overset{\mathrm{m}}{.}25$ and $(U-B) = 0\overset{\mathrm{m}}{.}07$ correspond to those of an unreddened A8 V star with $T_{\rm eff} = 7\,600$ K. Our observations revealed that in addition to the far–IR excess, the star shows an excess in the

Table 5. $UBVRI$ photometry of HD 36112. The Julian dates are given with the offset of 2400000.

JD	V	$(U-B)$	$(B-V)$	$(V-R)$	$(V-I)$
48996.21	8.37	0.06	0.24	0.24	0.44
48997.18	8.38	0.09	0.26	0.28	0.50
48998.16	8.36	0.12	0.24	0.25	0.45
49403.13	8.42	0.08	0.24	0.35	0.65
49423.13	8.33	0.00	0.26	0.27	0.52
49427.12	8.38	0.02	0.24	0.28	0.51
49605.43	8.35	0.05	0.15	0.21	0.47
49610.45	8.24	0.07	0.21	0.27	0.47
49729.18	8.33	0.05	0.28	0.34	0.66
49740.13	8.31	0.08	0.24	0.24	0.39
49741.17	8.31	0.05	0.29	0.22	0.43
49742.18	8.38	0.11	0.29	0.31	0.54
49803.14	8.32	0.11	0.25	0.25	0.51
49804.11	8.31	0.11	0.26	0.25	0.44
50093.23	8.35	0.10	0.25	0.26	0.47
50096.22	8.35	0.00	0.28	0.22	0.37
50097.23	8.28	0.07	0.27	0.25	0.45
50101.17	8.31	0.12	0.28	0.30	0.59
50107.27	8.36	0.09	0.26	0.25	0.47
50347.50	8.34	0.10	0.28	0.31	0.50
50416.29	8.31	0.09	0.26	0.26	0.45
50426.41	8.34	0.10	0.28	0.28	0.38

Table 6. JHKL photometry of HD 36112

JD2400000+	J	H	K
*	7.44	6.70	5.90
49059.31	7.37 ± 0.03	6.75 ± 0.02	5.91 ± 0.03
49062.26	7.41 ± 0.02	6.78 ± 0.02	5.95 ± 0.02
49729.20	7.15 ± 0.09		6.17 ± 0.02
49740.13			5.94 ± 0.13
50093.23	7.15 ± 0.13	6.80 ± 0.06	5.88 ± 0.04
50096.22	7.32 ± 0.18	6.68 ± 0.03	6.05 ± 0.20
50101.17	7.30 ± 0.13	6.65 ± 0.05	5.72 ± 0.04
50107.27	7.23 ± 0.04	6.66 ± 0.12	5.86 ± 0.13
50347.50	7.25 ± 0.18	6.66 ± 0.10	5.79 ± 0.14

* Observations by Bogaert (1994), who also quoted the L'-magnitude of HD 36112 (at 3.8 μm) being $4\overset{\mathrm{m}}{.}74$, while our observations taken on JD2449062.26 in the L passband (centered at 3.5 μm) gave the value of $4\overset{\mathrm{m}}{.}98 \pm 0\overset{\mathrm{m}}{.}07$.

near-infrared region (Fig. 1a). Such a behaviour is similar to that of young Herbig Ae/Be stars.

4.2. Spectral type estimates

The effective temperature and surface gravity of HD 36112 were derived from a comparison of the theoretical and observed colour indices in the Strömgren-Perri system. We used a traditional method of stellar atmosphere analysis, which was described by Savanov (1995). It should be noted that a study of rapidly rotating stars with $V \sin i > 30 \div 40\,\mathrm{km\,s^{-1}}$ is hampered by strong blending of spectral lines and is possible only involving the comparison with theoretical spectra. Calculations were based on the Kurucz (1979) stellar atmosphere models and performed with the use of the code analogous to that described by Liubimkov (1986). As a result, the following values were derived: $T_{\rm eff} = 7\,700 \pm 200$ K, $\log g = 4.00 \pm 0.25$. Their accuracy is mainly determined by the variability of the colour-indices, which is close to the accuracy of our photometry (see Sect. 4.1).

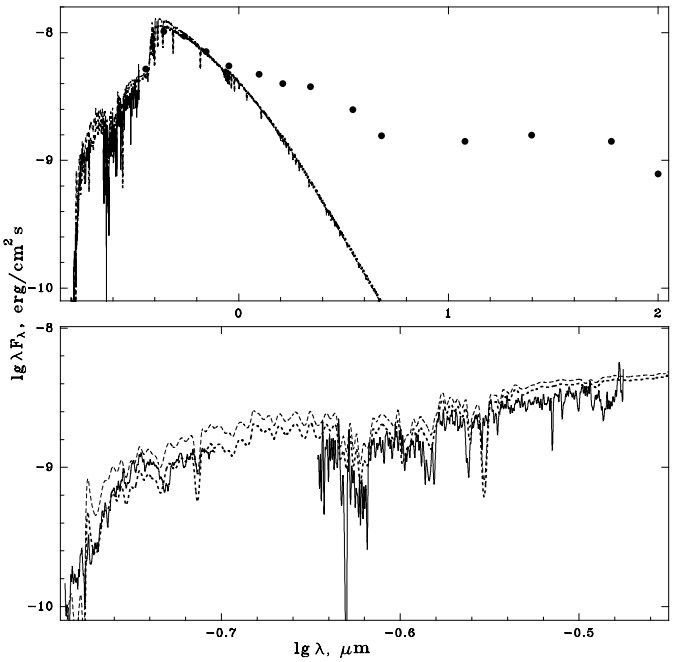

Fig. 1. Observed spectral energy distribution of HD 36112, constructed using the IUE low-dispersion spectra (LWP 30023 and SWP 53939), shown by a solid line, and the photometric data contained in this paper, together with the *IRAS* fluxes (filled circles): in the range 0.1–100 μm (*top*), in the IUE region (*bottom*). Also shown are Kurucz (1994) models for $\log g = 4.0$, $T_{\rm eff} = 7\,500$ K (dotted line) and $T_{\rm eff} = 7\,750$ K (dashed line).

The Hα and Hβ line wings, free of emission, were used for an independent estimate of the star's spectral type. Analysis of the theoretical line profiles (Kurucz 1979) revealed, that for $T_{\rm eff} \lesssim 8\,000$ K the wings are very sensitive to temperature, and for $T_{\rm eff}$ in the interval $7\,000 \div 8\,500$ K they are not sensitive to gravity. The best agreement between the observed and computed profiles was achieved for $T_{\rm eff} = 7\,600$ K, which coincides with the photometric estimate. Comparison of the observed UV flux distribution with that of the Kurucz (1994) models (Fig. 1) completely confirms the above estimate of $T_{\rm eff}$. Thus, we can conclude that HD 36112 is an unreddened A8 V star.

4.3. Binarity checking

All unblended photospheric lines with known laboratory wavelengths observed during four observational seasons (see Table 3) were used to search for positional variations which could be a consequence of the system binarity. The mean heliocentric ve-

locity of HD 36112 (with the scatter of individual values not exceeding the errors) was derived as $+17.6 \pm 0.2\,\mathrm{km\,s^{-1}}$. This result excludes the hypothesis about the object's binarity.

4.4. Projected rotational velocity

$V \sin i$ was derived by means of several iterations simultaneously with $T_{\rm eff}$ and $\log g$ determination (see Sect. 4.2). All the lines listed in Sect. 2.1 were used. Line broadening was accounted for by means of a method described by Liubimkov (1986). The absence of noticeable veiling and apparent symmetry of photospheric lines allowed to estimate the projected rotational velocity with sufficient accuracy. The ultimate value of $V \sin i$ is $60 \pm 6\,\mathrm{km\,s^{-1}}$.

4.5. Chemical anomalies

The abundances of five elements in the atmosphere of HD 36112 have been derived from the comparison of the theoretical and observed spectra:

O	:	$8.7 \div 8.9$	
Si	:	8.0	
Ca	:	6.3	
Fe	:	7.5	
Ba	:	2.6	$\lambda_c = 6160$ Å
Ba	:	2.9	$\lambda_c = 6400$ Å
Ba	:	2.4	$\lambda_c = 5854$ Å

The abundances of iron, calcium, and oxygen do not differ significantly from those of the Sun. The excess of silicon (~ 0.4 dex) was derived on the basis of data on the lines at $\lambda\lambda$ 6347 and 6371Å. The abundance of Ba was found to exceed the solar value by ~ 0.6 dex. Its maximum value was determined from the BaIIλ 6497 Å line. However, as was mentioned by Savanov (1995), this line is a complex blend in the stars with rotational velocity exceeding $40\,\mathrm{km\,s^{-1}}$ and is distorted by telluric water vapour lines. To our mind, the most reliable estimate is based on the analysis of the line at λ 6141 Å, which is the most frequently used to determine the abundance of barium in chemically peculiar stellar atmospheres.

4.6. Circumstellar lines

The Hα profiles observed in different runs are rather diverse in type (Fig. 2). As a wellknown Herbig A0e star AB Aur (Beskrovnaya et al. 1995), HD 36112 displays a classical P Cyg II profile (24/25.12.1994, January 1996), P Cyg III profile (29–31.12.1994, 6/7.01. and 5/6.11.1995), and a single peak without P Cyg absorption (in February–March 1995). The Hα emission was observed blueward up to $-400 \div -300\,\mathrm{km\,s^{-1}}$, and redward – up to $+280 \div +420\,\mathrm{km\,s^{-1}}$ (Table 1).

The He I emission line at λ 5876 Å shows a single symmetric profile which is blueshifted on the majority of dates (between 0 and $-130\,\mathrm{km\,s^{-1}}$).

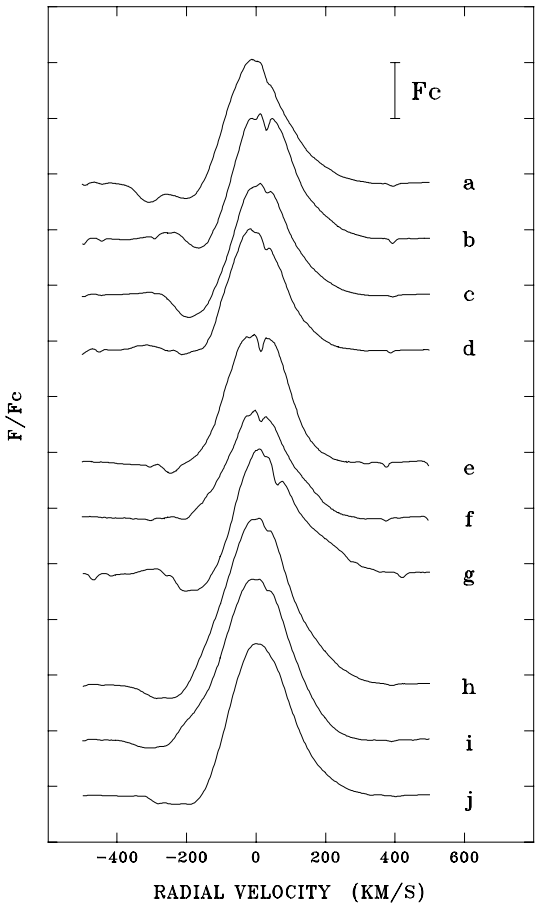

Fig. 2. Nightly mean Hα profiles observed in HD 36112 on the following dates: a) 24/25.12.94; b) 29/30.12.94; c) 30/31.12.94; d) 6/7.01.95; e) 25/26.02.95; f) 4/5.03.95; g) 5/6.11.95; h) 9/10.01.96; i) 10/11.01.96; j) 11/12.01.96. The radial velocity scale is given with respect to the star. No attempt has been done to remove water vapour lines.

The width of the He I λ 5876 profile is somewhat narrower than that of Hα: from –350÷–200 up to +200÷+300 km s^{-1} (Table 2, Fig. 3).

The most unusual appears the DNa I emission doublet. D_1 and D_2 lines have P Cyg II profiles with the blue edges at almost the same velocities as that of the Hα in all the spectra. Emission peaks are blueshifted from –15km s^{-1}(29/30.12.94) to –50km s^{-1}(30/31.12.94). However, their red edges are located at +100÷+150km s^{-1}(Table 2). In addition, the narrow absorption components of variable intensity, but with the constant redshift $+4 \pm 1\,\mathrm{km\,s^{-1}}$, are present in the lines (Fig. 3). The central intensity of the D_2 line was 0.49 in December, 1994–January, 1995 and 0.63 in January, 1996. At the same time, the ratio of central intensities of the D_2 and D_1 lines was constant (1.35 ± 0.05) and was in agreement with the oscillator strengths ratio, $f_2/f_1 = 1.33$.

In December, 1994–January, 1995 correlated positional changes of the central emission peaks were observed from date to date: from -10 to $+25\,\mathrm{km\,s^{-1}}$ in Hα, from -50 to $-15\,\mathrm{km\,s^{-1}}$ in D Na I, and from -130 to $0\,\mathrm{km\,s^{-1}}$ in

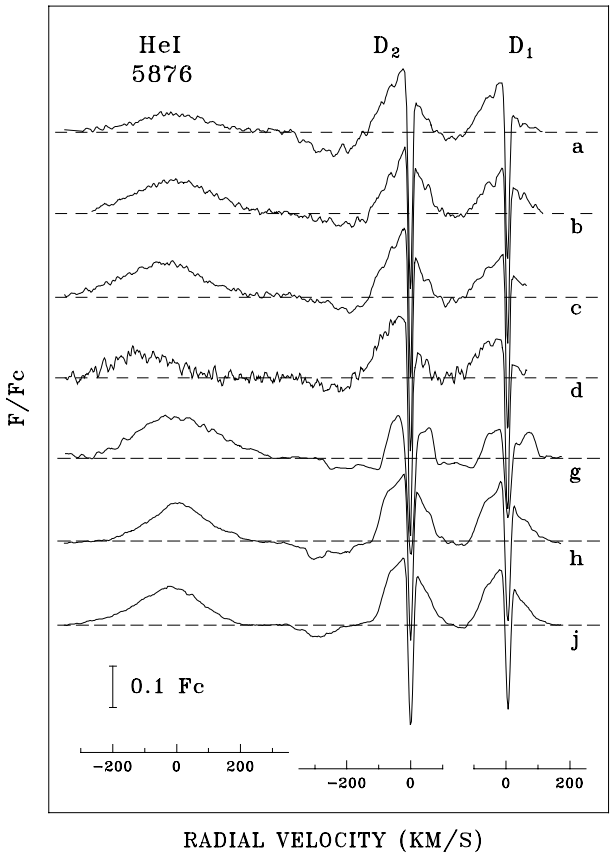

Fig. 3. The same as Fig. 2, but for He I λ 5876 and DNa I lines. The telluric lines are removed from all the spectra.

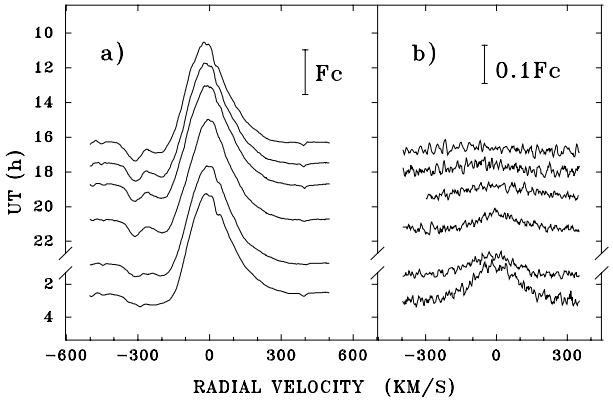

Fig. 4a and b. Rapid variations of the Hα and He I λ 5876 line profiles observed during the night 24/25.12.94

He I λ 5876 Å. During other observing runs this type of variability was not observed (Tables 1, 2).

Rapid variations during a night were observed in all circumstellar lines. The majority of them look like local monotonous intensity changes in different parts of the profile without positional shift of changing details. The same type of rapid variability of the Herbig Ae/Be stars was reported by Pogodin (1994) in HD 163296 and Beskrovnaya et al. (1995) in AB Aur.

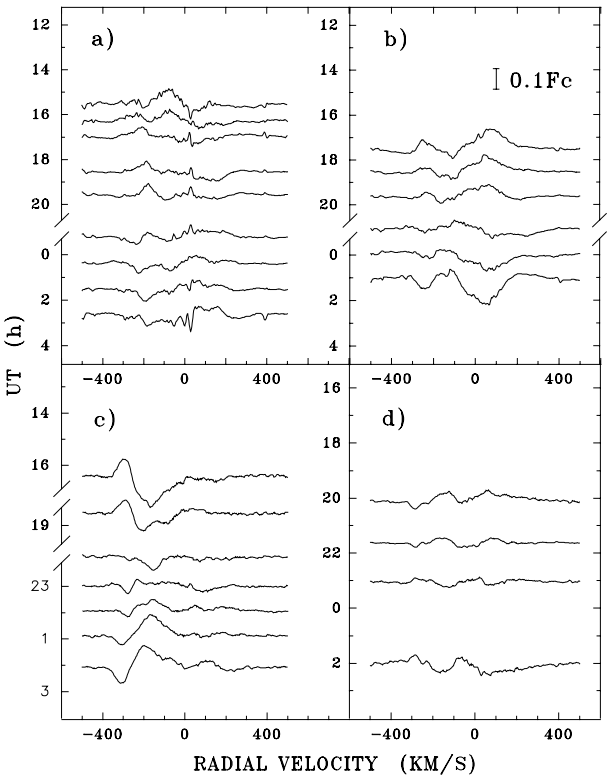

Fig. 5a–d. Residuals with respect to the nightly mean Hα profiles observed in HD 36112 on the following dates: **a** 29/30.12.94; **b** 30/31.12.94; **c** 9/10.01.96; **d** 10/11.01.96

4.7. Rapid variability of circumstellar lines in different runs

Fig. 4 presents the picture of the Hα and He I λ 5876 line profiles changes during the night 24/25.12.1994. One can notice a monotonous increase of intensity in the He I λ 5876 line, while two P Cyg absorption components of Hα (centered at -200 and $-300\,\mathrm{km\,s^{-1}}$) gradually converged and finally formed one broad absorption feature.

Rapid variability of the Hα profile during other observing nights is shown in Fig. 5, which presents the residuals constructed with respect to the nightly mean spectrum. A number of variable but positionally stable features are clearly seen as 'standing waves' close to the line centre and in the region of negative velocities up to $-400\,\mathrm{km\,s^{-1}}$.

In January 1996 (Fig. 5c, d) the most clearly seen changing details centered at -300 and -200km s^{-1} were observed in both the Hα and DNa I lines (Fig. 6).

4.8. Polarization features

As has been noticed by a number of authors (see, e.g., Shakhovskoy 1994 and references therein), a correct statistical analysis of the polarimetric observations can be performed only in terms of the Stokes parameters Q, U (or q, u), rather than using the polarization degree, P% and the position angle θ°. This is connected with the fact, that the latter do not fit

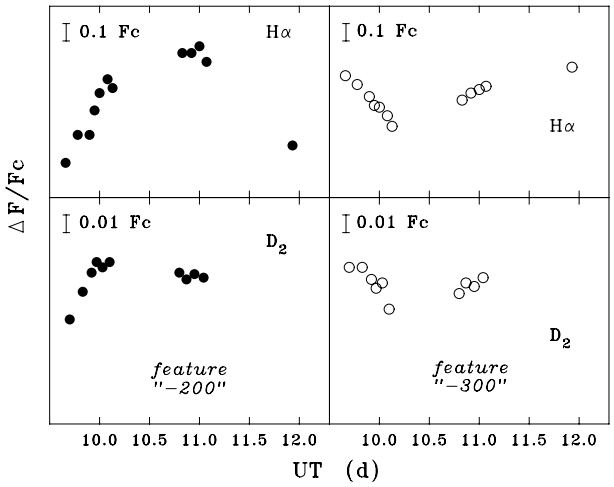

Fig. 6. Relative intensity variations of the "−200" (•) and "−300" (○) local features on the profiles of the Hα and D_2 lines in January, 1996

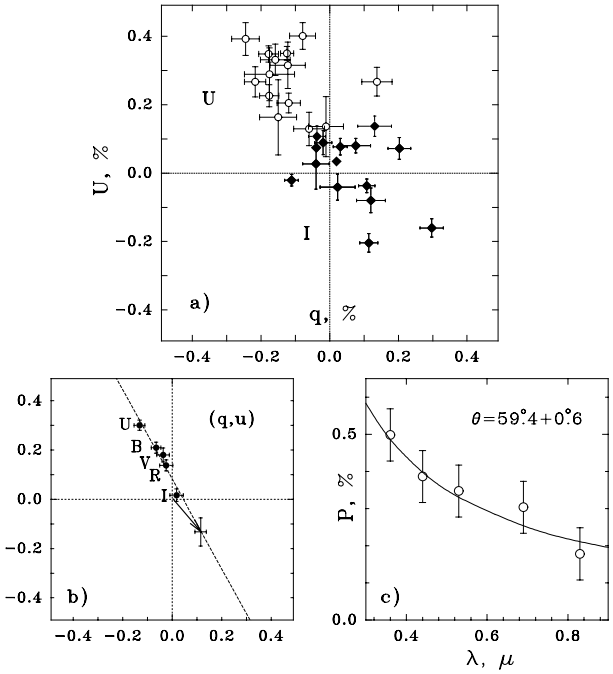

Fig. 7. a The nightly mean values of the q and u parameters of HD 36112 for all observing dates in the U (open circles) and I (filled circles) passbands. **b** The Stokes parameters of HD 36112 in different passbands averaged for all observing nights (filled circles). The arrow and the dashed line indicate the vector of non-selective component and the direction of the selective component vector (the same in all the passbands), respectively. **c** The wavelength dependence of the selective component. The line is drawn for the law $P(\lambda) \propto \lambda^{-1}$.

the normal distribution, and thus their mean values cannot be regarded as the unshifted estimates of the real values.

The observed normalized Stokes parameters of HD 36112 demonstrate a striking variability from date to date. On the (q, u)-plane the nightly mean values for each passband form a cloud of points with the radius of scattering up to 0.4%, which exceeds the errors of individual points by an order of magnitude. The positions of these clouds on the (q, u)-plane exhibit a conspicuous wavelength dependence (Fig. 7a). The points corresponding to the weighted mean values for all the data in each passband are situated along a straight line (Fig. 7b). This allows to distinguish (by means of the least-squares method) two constant background components of polarization: a non-selective component with $P = 0.18\%$ and $\theta = 156° \pm 3°$ (Fig. 7b), and a selective one with $P(\lambda) \propto \lambda^{-1}$ and $\theta = 59\overset{\circ}{.}4 \pm 0\overset{\circ}{.}6$, shown in Fig. 7c.

Variations in different passbands are strongly correlated, thus giving evidence of their reliability. They seem to be not wavelength dependent, since the radius of scattering is the same in all five clouds.

5. Discussion

5.1. Chemical anomalies and evolutionary status of HD 36112

In order to understand the origin of chemical anomalies in the atmospheres of chemically peculiar (CP) early type stars, it is very important to determine when they arise – during the PMS evolution of a star, or after a star has reached the ZAMS. In order to answer this question, it is possible, for instance, to study CP stars belonging to clusters of different ages. Although such studies have been performed by a number of authors (see, e.g., the review by Nort 1993), the time of arising of chemical anomalies can be determined directly only by investigating the atmospheres of PMS stars.

The distance to HD 36112 derived from the HIPPARCOS parallax (ESA 1997), $r = 200 \pm 50$ pc, allows to estimate the age of the object, using the evolutionary tracks in the $\log L_{\rm bol}/\log T_{\rm eff}$ diagram by Palla & Stahler (1993). The most probable values for the mass and the age of HD 36112 turn out to be: $M/M_{\odot} = 1.8 \pm 0.2$ and $t = 5 \div 10 \times 10^6$ years, that means, that the star is still at the PMS phase of evolution, but close to the ZAMS.

The SED of HD 36112 (Fig. 1a) is 'flat', rather than 'double-peaked' in the IR region, that is typical for younger Herbig stars (Waelkens et al. 1994), and is very similar to that of AB Aur, whose age is estimated as 3×10^6 yr (van den Anker et al. 1998).

The anomalous abundances of barium and silicon, which have been found in HD 36112 (see Sect. 4.5), are similar to those common for CP stars situated in an upper part of the MS, in particular, for a number of "metallic" stars (Savanov 1995).

The origin of chemical peculiarities is now commonly believed to be connected with the process of diffusion of different elements in stellar atmospheres. According to Charbonneau & Michaud (1988, 1990), the diffusive separation of elements can occur even in the atmospheres of stars with significant rotational velocities (up to 100 km s^{-1}). On the other hand, Michaud et al. (1983) pointed out that the influence of the mass-loss processes can be even more important. As it was shown by Alecian (1990), significant changes in the mass-loss rates can result in anomalies of a different sign, from deficit to excess. All mentioned above allows to suggest that chemical anomalies can arise already during the early (PMS) stages of stellar evolution. This

suggestion is supported by the discovery of chemical anomalies in HD 36112.

5.2. Circumstellar envelope of HD 36112

The results of our observations make it possible to discuss some important points on the structure and kinematics of circumstellar envelope around HD 36112:

1. P Cyg-profiles observed in the Hα and DNa I lines imply that the stellar wind is the main component of the gaseous envelope. The fact that radial velocities observed in the Hα profile are higher than those in the He I λ 5876 profile means that the maximum wind velocity is achieved in more remote regions than the high-temperature zone. At the same time, very high velocities observed in the DNa I lines, which on some dates reach the same values as those in the Hα, show that $V_\infty \sim V_{max}$. Such a situation can occur only if the region of circumstellar gas acceleration is rather extended.
2. A striking asymmetry of the DNa I lines with dominating blue component can be caused by the existence of an extended outer gaseous envelope, which screens the receding part of the wind. This assumption is confirmed also by the observed variations of the narrow absorption features in the DNa I profile, which may be of both interstellar and circumstellar origin.
3. This opaque gaseous envelope is likely to be an inner part of the extended gaseous-dusty disk surrounding HD 36112. In spite of the fact, that the orientation of the envelope has to be close to 'edge-on' (according to our spectroscopic data), the disk seems to be inclined relative to the line-of-sight and to have an inner gap. This results in the absence of screening the star by the circumstellar matter. The following facts speak in favour of this assumption:
   – A large IR excess is present in the SED, while the IS/CS reddening is practically absent in the optical and UV spectral ranges (see Fig. 1).
   – No manifestations of photometric variations with a peak-to-peak amplitude exceeding $0\overset{\mathrm{m}}{.}2$ have been observed.

   Analysis of the polarimetric data (see Sect. 4.8) revealed the presence of at least two polarization components, connected with scattering on circumstellar dust (interstellar scattering is likely to be negligible, since no reddening is observed). It is remarkable, that the vectors corresponding to the selective and non-selective components (Fig. 7b) have practically the opposite directions in the (q, u)-plane, thus giving evidence that the sources of these polarization components (that is, the large-grained and small-grained dust) are situated in the orthogonal planes. Taking into account that small-grained dust is more likely to be swept by the radiation pressure, we can assume that the large-grained dust is more concentrated towards the polar regions, while the small-grained dust survive in the equatorial regions, where screening of stellar radiation by dense equatorial disk may occur.
4. The combined spectroscopic and polarimetric evidences allows to conclude about the presence of azimuthal inhomogeneities in the circumstellar envelope of HD 36112. A number of them are presented in the next subsection.

5.3. Azimuthal inhomogeneity of the circumstellar envelope

5.3.1. Spectroscopic evidences

An appearance of positionally stable but variable in intensity local features at high negative velocities looks like a paradox, since these parts of the emission line profiles are formed in the fast moving gaseous medium. Only two possible hypotheses can be suggested to explain this phenomenon:
a) Due to any kind of hydrodynamic phenomena there appear gaseous condensations slowly moving with respect to the star and to an observer. Slowly precessing condensations of this type are known to form in the envelopes of rapidly rotating classical Be stars – so called "one-armed" perturbations (Okazaki 1991). Up to date there is no theoretical or observational evidence for existence of such structural features in the envelopes of PMS stars.
b) In the gaseous envelope there exist long-lived outflowing streams rotating around the star. It is not difficult to show, that the surfaces of equal radial velocities are oriented perpendicularly to the line-of-sight between the star and an observer, and a rotating jet is moving along these surfaces in front of the star.

We have tested this effect using the model of an envelope with a rotating gaseous jet (Pogodin 1990). Calculations have shown that when the jet is moving close to the line-of-sight, positionally stable local features appear in the region of negative radial velocities, exhibiting intensity variations on the time scale of hours. Observational evidence of such long-lived outflowing streams has been reported for AB Aur (Beskrovnaya et al. 1995).

As was mentioned in the paper by Beskrovnaya et al. (1998), devoted to the investigation of another well-known Herbig Ae star HD 163296, if azimuthal inhomogeneities are present in a gaseous envelope of a single star, the following phenomena can be observed:

1. Counter-phase changes in the red and blue emission wings of the envelope lines. In the objects with a strong stellar wind this type of variability can be connected with the movement of azimuthal inhomogeneities close to the line-of-sight.
2. Positional changes of the emission peak of the envelope lines. They should arise during the passage of a rotating inhomogeneity through the sky plane.

If the lifetime of a gaseous jet exceeds several spin periods, cyclic variations of different profile parameters with the period of the envelope rotation in the region of the jet formation can be expected.

Since no signs of binarity have been observed in HD 36112 (see Sect. 4.3), the above criteria can be applied to this object for a diagnostics of large-scale azimuthal inhomogeneities.

According to both of them, such inhomogeneities should exist in the gaseous envelope of HD 36112. Fig. 8 shows the changes of the blue (V_b) and red (V_r) edges of the Hα emission

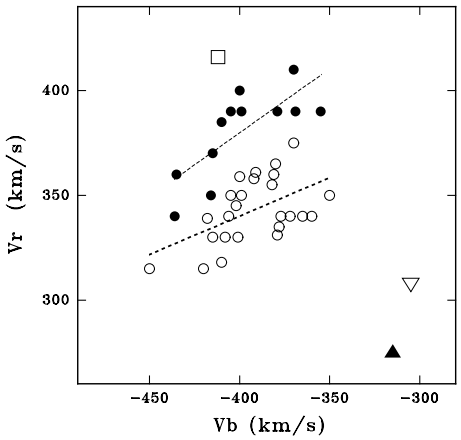

Fig. 8. The velocity positions of the blue ($V_{\rm b}$) and red ($V_{\rm r}$) emission limits of the Hα line for different observing seasons: December 1994–January 1995 (open circles); February, 25/26 1995 (filled triangle up); March, 4/5 1995 (open triangle down); November, 9/10 1995 (open square); and January 1996 (filled circles).

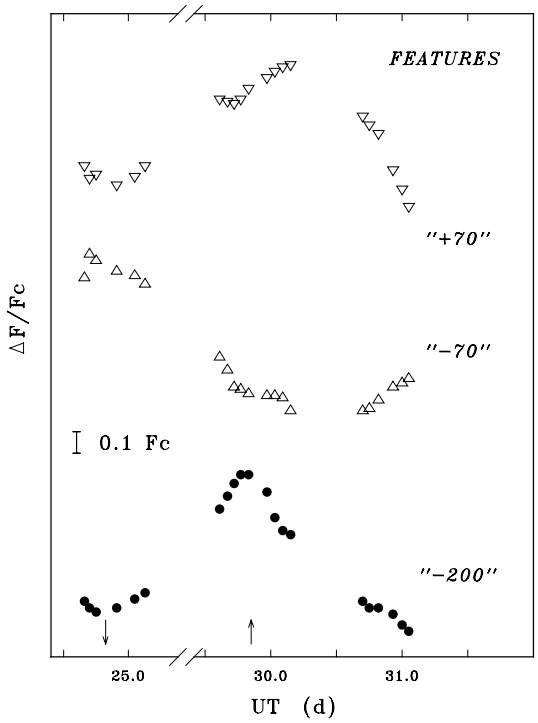

Fig. 9. Variations of the relative intensities for the local features on the Hα profile centered at $V_{\rm r} = -200\,{\rm km\,s^{-1}}$ ("-200"), $V_{\rm r} = -70\,{\rm km\,s^{-1}}$ ("-70"), $V_{\rm r} = +70\,{\rm km\,s^{-1}}$ ("$+70$") in December, 1994 – January, 1995. The positions of expected minimum and maximum for the period $P = 48^{\rm h}$ are marked by arrows.

profile for all observing runs. Anti-correlation character of these variations during the runs December, 1994–January, 1995 and January, 1996 is clearly seen. As was mentioned in Sect. 4.6, positional shifts of the central emission peaks of the Hα, He I λ 5876 and DNa I lines have been also observed in December, 1994–January, 1995.

In more detail the phenomena observed during this season can be analyzed with the use of residuals, constructed for all individual spectra taken on December, 24/25, 29/30 and 30/31 1994, with respect to the mean spectrum for the whole run. Positional shifts of the emission peak, which are given in column 4 of Table 1, manifest themselves in the residuals in the form of counter-phase variations of relative intensity of local spectral features at the opposite low ($+70/-70\,{\rm km\,s^{-1}}$) velocities. The width of these features is, as a rule, of the order of $100\,{\rm km\,s^{-1}}$. Fig. 9 presents variations of the relative intensities for these local features as well as for the feature at $V_{\rm r} = -200\,{\rm km\,s^{-1}}$ (marked as "-70", "+70", and "-200" respectively) during three nights. As it was discussed earlier (Sect. 4.7), their positions are almost unchanged during a night except for the small night-to-night shifts not exceeding half of their widths. So, the intensity of the features was measured at the velocities corresponding to the maximum amplitude of the variations for each night.

The curves look like fragments of a sinusoid with a period of about 2 days, the amplitude in the range $0.6 \div 0.8 F_{\rm c}$ and phase shifts expected within a simple kinematical model of a rotating azimuthal inhomogeneity provided the orientation of the envelope is close to 'edge-on'. Really, the maximum intensity of the "-70"–feature corresponds to the position of a jet-like inhomogeneity, when it is moving towards an observer after the passage of the sky plane. The maximum intensity of the "-200"–feature is to be observed, when the jet is close to the line-of-sight, and of the "+70"-feature – when it is moving away from an observer and approaching the sky plane. In this case the intensity of the "+70"–feature changes in counter-phase with that of "-70"-feature, and its maximum should be observed with a delay of $P_{\rm rot}/4$ with respect to the maximum of the "-200"–feature, just what is seen in Fig. 9.

5.3.2. Polarimetric evidences

Investigation of the polarization parameters variations provides information on the presence and properties of circumstellar inhomogeneities.

A detailed analysis of our polarimetric data is rather complicated due to uneven data sampling. Nevertheless, the only continuous series of observations performed in January 1996 allows to draw some conclusions on the sources of the variable polarization component.

In all the passbands the variations are characterized by long-term trends and rapid changes during a night. The trends can be approximated by polynomials of the first (for the q–parameter) and the second (for the u–parameter) order. Fig. 10a illustrates variations of the q and u parameters in the B-passband during four consecutive nights (January 9–12, 1996) averaged on 1-hour intervals. The long-term trend, shown in Fig. 10a by solid line, has a form of the arc in the (q, u)-plane (Fig. 10b *right top*).

As it is seen in this figure, the rapid variations of the q and u parameters during a night has a clear counter-phase character. The correlation coefficient of the residual variations, calculated with respect to the nightly mean values (for three of the four nights when several observations were obtained) turned out to

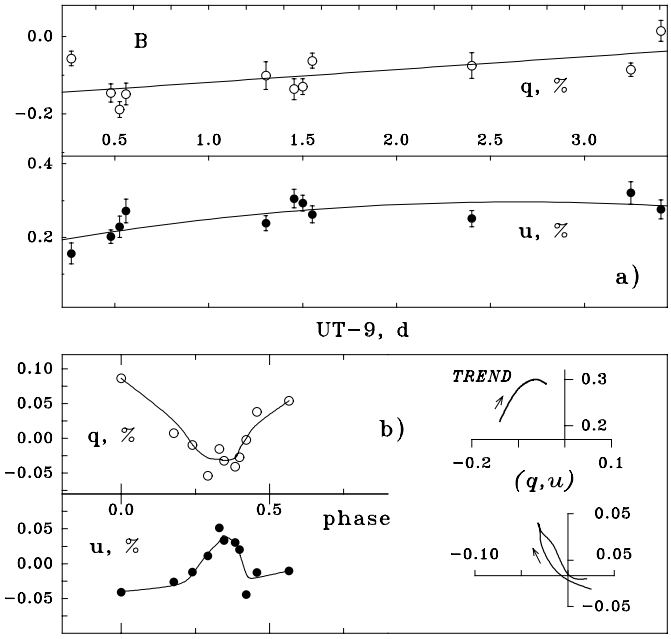

Fig. 10. a Variations of the polarization parameters of HD 36112 observed in the B-passband in January 9–12, 1996. The best fitted polynomial is shown by solid line. **b** Phase diagrams of the q, u parameters from the data of January 9–12, 1996 constructed for $P = 21^{\rm h}$ (*left*). The (q, u)-traces for the trend (*top*) and for the rapid cyclic variations (*bottom*) are presented in the right part of the figure. Arrows indicate the direction of phase increasing.

be $r = -0.73 \pm 0.14$. The similar values were derived for the residuals calculated by subtraction of the long-term trends approximated by first-order ($r = -0.71 \pm 0.15$) and second-order ($r = -0.64 \pm 0.16$) polynomials. In all cases the correlation coefficients are large enough that favors reliability of the observed rapid polarimetric variations. In the (q, u)-plane rapid variations will occur in the direction, which coincides with the direction of the selective background component of the polarization (see Fig. 7b). Thus one can assume that their origin is connected with processes in the equatorial plane of the circumstellar envelope. Non-selective character of the rapid variations may be connected with orbital movement of gaseous inhomogeneities near the star rather than with the small-grained dust in the outer regions of the envelope. In this case one can expect that this variability would have a cyclic character.

The application of the Laefler–Kinman (1965) method implemented in the computer code by Pelt (1980) to the whole q and u set obtained in 1996 January, 9–12 (129 observations in total, see column 2 in Table 4) resulted in the close values of the expected periods for both parameters ($P = 0\overset{\rm d}{.}90 \pm 0\overset{\rm d}{.}02$ for q and $P = 0\overset{\rm d}{.}86 \pm 0\overset{\rm d}{.}01$ for u). One should be careful considering these values because of uneven distribution of the data points on the period phases. However they turned out to be close to half the rotation period of the star ($\sim 1\overset{\rm d}{.}8$), which is expected for the parameters quoted in Sects. 4.2 and 5.1 and orientation close to 'edge-on'. Phase diagrams constructed for a mean period of $0\overset{\rm d}{.}88$ (Fig. 10b *left*) have been smoothed and plotted at the (q, u)-plane. The resulting trace (Fig. 10b *right bottom*) has a form of flattened loop oriented in the same direction as the background selective component (see Fig. 7b, Sect. 4.8). The direction of moving along the trace is the same as that for the long-term trend.

All above mentioned is in good accordance with the hypothesis about the orbital motion of different circumstellar inhomogeneities rotating in the common flattened gaseous–dusty envelope. In particular, the arc of the long-term trend can be suspected to be a part of the closed curve of the same orientation, reflecting the orbital movement of a remote condensation. The rapid polarimetric variations during four nights can be connected with rotation of a jet-like inhomogeneity with the orbital period $P \sim 1\overset{\rm d}{.}8$. The latter estimate is based on the fact, that non-magnetized rotating inhomogeneities exhibit polarimetric period equal to $0.5 P_{\rm rot}$.

This value of the expected orbital period is smaller than that fitting variations of the local features on the Hα profile, described in the previous paragraph. If this variability is caused by the orbital movement of azimuthal inhomogeneities, the region of their formation should be farther from the star, where the rotational velocity of the envelope is smaller. Nevertheless, we consider this result as a preliminary one, which should be confirmed on a more extended data set to be obtained in the future.

Thus, the results presented here speak in favour of the conclusion that circumstellar azimuthal inhomogeneities can form at different distances to the star, rather than only close to the photosphere. Their appearance seems to be connected with peculiarities of dynamical processes in the envelope and/or with stellar/circumstellar magnetic fields.

6. Conclusions

The results of a complex programme of spectral, polarimetric, and photometric study of the Ae star HD 36112 have shown that in addition to the far-IR excess, this star exhibits many properties common with young Herbig Ae/Be stars. The most important of them are as follows:

1. near–IR excess due to the presence of hot dust;
2. the presence of a high-temperature (probably chromospheric) zone responsible for the observed He I λ 5876 line;
3. 'global' variability of the Balmer line profiles passing through the stages P Cyg II– P Cyg III– single-peaked profile;
4. a peculiar type of rapid variability of the circumstellar line profiles probably connected with formation of circumstellar jet–like inhomogeneities at different distances to the star;
5. variable multi-component polarization parameters and irregularly-variable brightness;
6. an existence of a flattened dusty–gaseous circumstellar envelope;

Acknowledgements. We are grateful to Drs. F. Palla and Yu.S. Efimov for useful comments. The research described in this paper was made possible in part by the ESO C&EE grant A–05–21 for acquisition

of necessary computer equipment. This work was sponsored by the INTAS under grant 93-2478-Ext.

References

Alecian G., 1990, In: Michaud G.,Tutukov A. (eds.) Evolution of stars: the photospheric abundance connection. Montreal, Canada, p. 11
van den Ancker M., de Winter D., Tjin A Djie H.R.E., 1998, A&A 330, 145
Bergner Yu.K., Bondarenko S.L., Miroshnichenko A.S., et al., 1988, Izvestia Glavn. Astron. Observ. v Pulkove 205, 142
Beskrovnaya N.G., Pogodin M.A., Scherbakov A.G., Tarasov A.E., 1991, Pis'ma v Astron. Zh. 17, 825
Beskrovnaya N.G., Pogodin M.A., Najdenov I.D., Romanyuk I.I, 1995, A&A 298, 585
Beskrovnaya N.G., Pogodin M.A., Yudin R.V., et al., 1998, A&AS 127, 243
Bogaert E., 1994, Thesis, University of Leuven
Charbonneau P., Michaud G., 1988, ApJ 327, 809
Charbonneau P., Michaud G., 1990, ApJ 370, 693
Dong Y.S., Hu J.Y., 1991, Chin. A&A 15, 275
ESA, 1997, The Hipparcos and Tycho Catalogues. ESA SP-1200
Herbig G.H., 1960, ApJS 4, 337
Herbst W., 1994, ASP Conference Series 62, 35
Huovelin J., Poutanen M., Tuominen I., 1986, Helsinki Univ. of Techn., Radio Lab. Report VS166, p. 18
Kurucz R.L., 1979, ApJS 40, 1
Kurucz R.L., 1994, CD ROM No.19, Smithsonian Astrophys. Observ.
Laefler J., Kinman T.D., 1965, ApJS 11, 216
Liubimkov L.S., 1986, Izv. Crimean Astrophys. Obs. 74, 3
Michaud G., Tarasick D., Charland Y., Pelletier C., 1983, ApJ 269, 239
Nadzhip A.E., 1986, Trudy GAISh (Proc. of the Sternberg Astron. Inst.), 58
North P., 1993, ASP Conference Series 44, 577
Okazaki A.T., 1991, Pub. ASJ 43, 75
Oudmaijer R.D., van der Veen W.E.C.J., Waters L.B.F.M., et al., 1992, A&AS 96, 625
Pelt J., 1980, In: Frequency Analysis of Astronomical Time Sequences. Tallinn, Valgus
Palla F., Stahler S.W., 1993, ApJ 418, 414
Perry C.L., Johnston L., 1982, A&AS 50, 451
Piirola V., 1975, Ann.Acad.Sci.Fennicae, Ser. AVI, Phys. N 418
Pogodin M.A., 1990, Astrofizika 32, 209
Pogodin M.A., 1994, A&A 282, 141
Pogodin M.A., 1995, Ap&SS 224, 539
Savanov I.S., 1995, AZh 72, 733
Serkowski K., 1974, N.Y.Acad.Press 12, Pt. A, 301
Shakhovskoy N.M., 1994, Izvestiya Crym. Astrophys. Obs. 91, 106
Thé P.S., de Winter D., Pérez M.R., 1994, A&AS 104, 315
Wackerling L.M., 1970, Mem.Roy.Astron.Soc. 73, 153
Waelkens C., Bogaert E., Waters L.B.F.M., 1994, ASP Conference Series 62, 405
Zuckerman B., Forveille T., Kastner J.H., 1995, Nat 373, 494

List of Objects

'HD 36112' on page 163
'MWC 758' on page 163
'AB Aur' on page 163
'CQ Tau' on page 163
'RR Tau' on page 163
'HD 32509' on page 163
'HD 35187' on page 163
'HD 31648' on page 163
'HD 163296' on page 171